Spatio-Temporal Reconstruction and Visualization of Plant Growth for Phenotyping

Jacket Demby's[1], Ali Shafiekhani[2], Felix B. Fritschi[3] and Guilherme N. DeSouza[4]

***Abstract*—Recently, there has been increasing interest in applying spatio-temporal registration for phenotyping of both individual and groups of plants in large agricultural fields. However, 3D non-rigid methods for registration are still a research topic and present numerous particular challenges in plant phenotyping due to: overlaps and self-occlusions in dense phyllotaxies; deformations caused by plant growth over time; changes in outdoor environmental settings, etc. In this paper, we address the problem of registering spatio-temporal 3D models of plants by proposing a bundle registration approach that can handle transformations with up to three additional Degrees of Freedom (DoF) to capture the growth of the plant. Besides, we offer to the research community a new multi-view stereo dataset consisting of 2D images and 3D point clouds of an African violet plant observed over a period of ten days. We evaluate the proposed algorithm on the new African violet dataset using the usual 6 DoF (three rotations and three translations) and compared it with 7 DoF (three rotations, three translations, and one scale) and 9 (three rotations, three translations, and three scales). We also performed the comparison between the proposed approach and two other registration approaches: pairwise and incremental. We show that the proposed algorithm achieves an average registration error of less than 2 mm on the African violet dataset. Also, we used VisND, an N-dimensional spatio-temporal visualization tool, to perform a visual assessment of the aligned time-varying 3D models of the plants.**

***Index Terms*—3D and 4D point clouds, plant phenotyping, spatio-temporal registration, 3D reconstruction, N-dimensional visualization**

I. Introduction

In order to understand plant development, plant scientists and breeders must be able to evaluate changes in anatomical, physiological, and biochemical properties over time [1], [2]. Plant phenotyping usually involves the continuous measurement, tracking, and monitoring of various plant traits, such as: leaf area, leaf leaf size, leaf color, stem length, plant architecture, canopy height, etc. However, these phenotypical properties are often obtained through manual, laborious, costly, and time-consuming methods. So, over the years, robotics and computer vision techniques have been employed in plant phenotyping to automate the process of measuring and evaluating multiple plant characteristics [3]–[5]. Most of these systems acquire 2D and 3D data from the scenes at different viewing angles [6]–[8], and while the data may be acquired using a variety of sensors – from simple RGB to time-of-flight (ToF), or even multi-spectrum cameras – all methods still require the registration of 3D models over space and time. Registering 3D models of an object consists of finding the transformation between corresponding 3D points in the source and target models in order to align their corresponding parts [9]–[11]. If the point clouds are such that Euclidean distances between every pair of points are preserved both in the source and target point clouds, a fixed and linear (i.e. *rigid*) transformation is sufficient to produce the registration of source and target models. On the other hand, if the relationships between pairs of points are not preserved, often multiple and/or non-linear transformations (i.e. *non-rigid*) are needed to register the two point clouds. In that sense, non-rigid 3D registration should be a fundamental component in the pipeline of any 3D computer vision techniques for plant phenotyping.

Fig. 1: (Left) Schematic representation of the 4D Scanner equipped with a (*stereo-rig camera*), a (*turn table*), two (*raspberry pi*) , and a (*LED lamp*). It can collect temporal 360^o view of the object. (Right) A sample stereo images: *top*, and *bottom images* captured by the 4D Scanner.

As we mentioned before, recent works [12]–[15] have already shown the need for temporal registration and visualization of multiple scans of 3D plants taken at different times to monitor the development of plants. These time-series based methods often need to acquire previously generated 3D point clouds of growing plants at different days, retrieve 3D information (keypoints, descriptors, skeleton, etc.), and perform optimization by iteratively aligning those point clouds to capture and monitor the deformations of different parts of the plants. The registration of 3D time-series point clouds of plants appears to be a challenging problem due to the anisotropic growth and overlapping of different parts of the plants [12]. Besides, the deformations that some parts of the plant undergo account for non-rigid registration, which is also

Jacket Demby's, Ali Shafiekhani and G. N. DeSouza are with the Vision-Guided and Intelligent Robotics (ViGIR) Laboratory in the Department of Electrical Engineering and Computer Science (EECS). Felix B. Fritschi is with the Division of Plant Science: all at the University of Missouri, Columbia, MO, 65211. (email: udembys@mail.missouri.edu[1], Ashafiekhani@mail.missouri.edu[2], FritschiF@missouri.edu[3], DeSouzaG@missouri.edu[4])

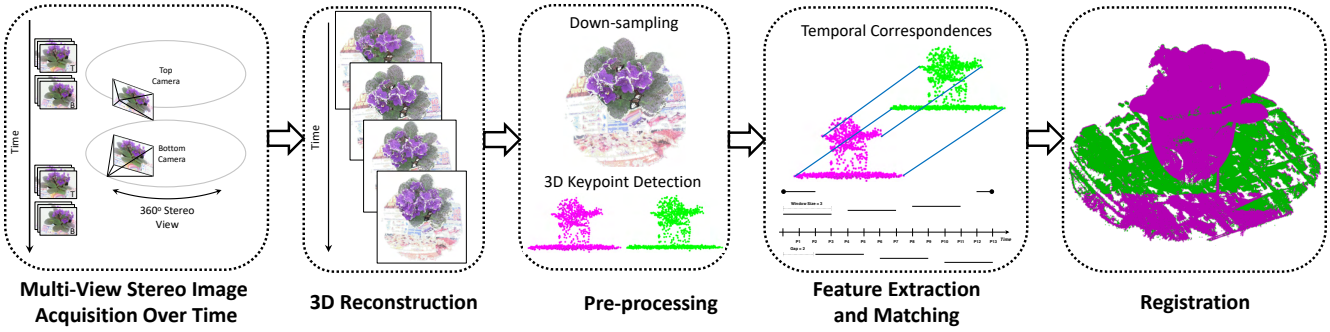

Fig. 2: The pipeline for the proposed method of spatio-temporal registration. The source and target point clouds are respectively differentiated in violet and green colors.

known to be a challenging problem in the computer vision community [9].

This paper's main contribution is three-fold: (1) a publicly available multi-view stereo dataset for temporal registration. The dataset is made of raw images collected over ten days and processed 3D point clouds of an African violet plant. (2) an algorithm for bundle registration that takes into account scale information to align the temporal 3D point clouds. (3) the incorporation of this algorithm into a previously developed, open-source N-dimensional visualization tool (VisND) [15]. The algorithm optimizes the registration of two point clouds based on non-isometric non-rigid transformations with rotation, translation, and scale parameters. Furthermore, the performance of the proposed algorithm is discussed and evaluated for 6 DOF (three rotation and three translation parameters), 7 DOF (three rotation, three translation, and one scale parameters), and 9 DOF (three rotation, three translation, and three scale parameters) transformations.

The rest of the paper is organized as follows: section II provides a literature review of rigid and non-rigid registration methods, 3D computer vision, and temporal registration techniques applied to plant phenotyping. Section III presents the African violet dataset that was used in this paper and made publicly available for researchers. Section IV provides an overview of the proposed registration algorithm for 3D time-series point clouds of plants. Section V reports the experimental results obtained using the proposed registration approach. Finally, section VI concludes this paper with insights about future work.

II. Related Works

Over the past two decades, many computer vision techniques have addressed the problems related to the registration of three-dimensional clouds of points [9], [16]–[19]. This process aligns two point clouds taken at different time instances. Registration algorithms come handy in estimating the transformation that maps two point clouds and are often classified into rigid and non-rigid registrations. On the one hand, rigid registration assumes a rigid setting where point clouds are related by a rigid 6 DoF transformation that can be expressed only using rotation and translation parameters. Some of the widely used rigid registration algorithms are based on Singular Value Decomposition (SVD) [20], Principal Component Analysis (PCA) [21], Iterative Closest Point (ICP) [22]. The latter have been explored in variant forms for surface registration with non-linear ICP [23] and generalized ICP [24]. On the other hand, non-rigid registration allows more DoF to capture the deformations — non-linear or partial stretching, shrinking, change of shape, etc. — of the point clouds over time. In this group, variant forms of the ICP algorithm were extended to 3D registration tasks: non-rigid ICP [25]–[28]. Overall, the great progress in rigid surface registration and the development of a variety of sensors have encouraged the community to bring non-rigid registration problems in computer vision, computer graphics, robotics, medical imaging, and reverse engineering into focus [9], [16], [29].

Despite significant successes in the fields mentioned above, time-lapsed non-rigid registration methods applied to plant phenotyping are still in their infancy and present numerous challenges (overlap, self-occlusion, deformations, environmental settings, phyllotaxy, etc.) related to the development process of a variety of plants. Recently, foundations have been laid down for spatio-temporal non-rigid registration of 3D point clouds of plants to capture changes in structure and track various phenotypic traits over time [12], [14], [15], [30]–[32].

At the agriculture field level, Dong et al. [14] addressed the problem of time-lapse dynamic scenes to model, track, and monitor the continuous growth of plants in a peanut field. The resulting 4D — 3D reconstruction associated with additional temporal information — spatio-temporal model consisted of time-series 3D point clouds registered with respect to a single global coordinate frame. While having an additional time dimension provides a richer representation of the field, it can be overwhelming for human to analyze and take advantage of the extra available information — growth rate, changing patterns, leaf color transition, etc. In that regard, Shafiekhani et al. [15] proposed an N-dimensional visualization tool named VisND for high-dimensional modeling and visualization of canopy for plant phenotyping. They created 5D models — 3D reconstruction, temperature, and time — of an agriculture field to study the behavior of plants in response to different

(a) Day 1 (b) Day 4 (c) Day 7 (d) Day 10

Fig. 3: A time-series of 3D point clouds of the same African violet plant captured during the blooming of its flowers processed using COLMAP [33], [34]. The proposed registration algorithm is able to capture its anisotropic growth, development and deformations over a 10-days period of time. For the different days, the presented clouds are obtained from raw 2D stereo images taken exactly at the same time 01:00 AM.

environmental conditions and stresses. Through its Graphical User Interface (GUI), VisND was then used to easily extract and analyze models registered over time.

At the individual plant level, Li et al. [31] proposed a 4D – 3D reconstruction and time — spatio-temporal framework based on a forward-backward analysis for growth event detection to address the challenge of accurately locating decay, budding and bifurcation of plants over time. Paproki et al. [32] introduced a mesh-based methodology to process mesh features, perform mesh morphological segmentation, tracking, and monitoring of individual plants over time. However, these works emphasized on obtaining the phenotypic traits of specific plant parts without the consideration of scale information when registering the time-lapse 3D point clouds. More recently, Chebrolu et al. [12] proposed a skeleton-based approach to track as well as register temporally separated 3D point clouds of individual plants. Their registration approach starts with the extraction of the skeletal structure of the point clouds, as described in [35]. This structure is then combined with a Hidden Markov Model (HMM) formulation to establish the correspondences between point clouds' pairs. However, their proposed registration algorithm was applied to a tomato plant for which skeletal information can easily be extracted, and did not take into account the scale deformations of the plants. Also, while building their dataset of the tomato plant, the authors minimized self-occlusion of the plant whenever possible and removed the noise points in a pre-processing step. Both steps allowed the algorithm to more reliably extract plant skeletons. In this paper, we focus on the time-lapse registration of 3D point clouds of a more challenging plant. We consider a growing African violet plant for which the blooming of its flowers was tracked over time.

III. Multi-view Stereo Dataset

We provide a real-world dataset of a growing African violet plant captured with a 4D scanner that we developed. As depicted in Figure 1, the 4D scanner is equipped with a stereo-rig camera (top and bottom cameras), a turntable, two Raspberry Pi, and an LED lamp to help the growth of the plant. The plant is placed on a turntable that rotates at specific time to allow the 4D scanner to capture stereo images over 360^o view of the plant. This data collection process was completely automated throughout the collection period. In fact, over a period of ten days, 194 sets of stereo images showing the blooming of the plant flowers were recorded and used to create dense 3D point clouds. A sample of stereo images (top and bottom images) is shown in Figure 1. The dataset, including both raw 2D images and processed 3D point clouds, is made publicly available for researchers in the field on this website[1].

IV. Methodology

In this section, an overview of the proposed method is described. Figure 2 shows the pipeline for spatio-temporal reconstruction using the dataset described in Section III. The pipeline starts with 3D reconstruction of images captured over 10 days. This step produces dense 3D point clouds of the plant at different timestamps (total 194 models). Next, a pre-processing stage is considered to reduce the size of the models and extract 3D keypoints representing important regions of the model. These 3D keypoints are then used to extract 3D feature descriptors. Using the extracted feature descriptors, correspondences between temporal models are found. We then use a bundle registration algorithm to register temporal models with respect to a global coordinate frame.

- **3D reconstruction**: We use COLMAP [33], [34] to process all the stereo images' sets and create 3D dense point

[1]http://vigir.missouri.edu/~dembysj/publications/SSCI2021/index.html

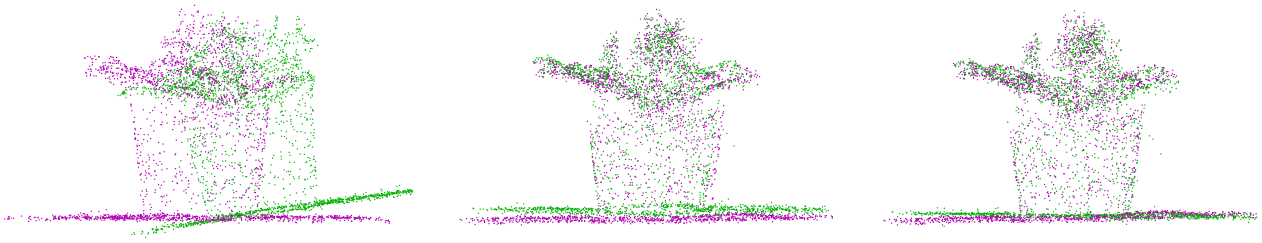

(a) PFH (b) FPFH (c) PFHRGB

Fig. 4: An example of the 3D registration of the same 2 consecutive point clouds from the violet dataset using *(a)* PFH, *(b)* FPFH and *(c)* PFHRGB taken from the same angle view while using the 7 DoF transformation. The source and target point clouds are respectively differentiated in violet and green colors.

clouds of the African violet plant. COLMAP is a general-purpose Structure-from-Motion (SfM) and Multi-View Stereo (MVS) pipeline with a graphical user interface that offers a wide range of features for 3D reconstruction tasks from multiple image sets. The top and bottom images were separated as they had different intrinsic parameters. Although camera calibration of the dataset is available, in this research we let COLMAP estimate intrinsic and extrinsic camera parameters. This is mainly to show effectiveness of the proposed algorithm for registration of models with different scales. We used default parameters of COLMAP with OpenCV camera model. In Figure 3, four typical reconstructed point clouds for days 1, 4, 7, and 10 captured at 1:00 AM are shown. In total, 194 point clouds of the plant over 10 days were reconstructed and provided with the publicly available dataset. The provided temporal models are all registered with respect to the same coordinate frame using the proposed registration method described next.

- **Preprocessing**: In this step, we downsampled the original 3D point clouds to speed up the computation. We empirically chose a leaf size of 0.01 for the results reported in this paper. We also extracted 3D keypoints to further speed-up the feature extraction and matching step. We used a 3D Harris operator [36] to detect keypoints on all the downsampled point clouds.
- **Feature extraction and Matching**: Looking at the literature, different 3D descriptors are introduced for different computer vision problems e.g. registration, seen recognition, object detection, etc [37]–[39]. Among these 3D feature descriptors, Point Feature Histogram (PFH) [40], Fast Point Feature Histogram (FPFH) [41] and Color Point Feature Histogram (PFHRGB) that was developed by the PCL community [42] are suited for 3D registration of point clouds. In that regard, a comprehensive review of 3D point cloud descriptors [38] showed that PFHRGB outperforms other descriptors for our registration task. In addition, we empirically evaluated these feature descriptors on the entire African violet dataset by varying the matching threshold, and PFHRGB which provided the best overall alignment results was retained in our methodology. Figure 4 shows a 3D registration example when trying to align the point clouds using the 3D feature descriptors mentioned above.
- **Normalization**: As mentioned before, to show effectiveness of the proposed registration algorithm, uncalibrated images are used in COLMAP during the 3D reconstruction step. As a result, COLMAP produced point clouds in different scales. As a preprocessing step, we apply a normalization step to help the registration discussed next. Equation 4 shows how the point clouds are normalized. Given an input point cloud P of size $3 \times N$ where the 3 dimensions represent (X, Y, Z) 3D coordinates of the vertices, we normalized each of the point clouds by applying the following equations:

$$\mu_i = \frac{\sum_{j=1}^{N} P_i(:, j)}{N} \tag{1}$$

$$P_{0_i} = P_i - \mu_i \tag{2}$$

$$s = \|P_{0_i}\| \tag{3}$$

$$P_{n_i} = \frac{P_i - \mu_i}{s} \tag{4}$$

where N is the number of vertices, μ_i is the center of the point cloud i and s is the scale. P and P_n are respectively the unnormalized and normalized 3D point clouds.

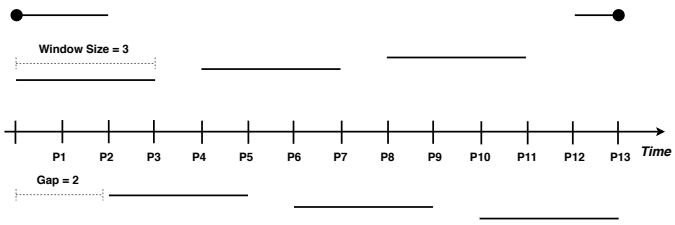

Fig. 5: Representation of bundles with sliding window and gap. At each bundle optimization, all models within the bundle are aligned with respect to the first model. Sliding this bundle optimization by a gap step smaller than window size ensures overlaps.

- **Bundle Registration**: We adopted a bundle registration approach to align all the temporal point clouds. At each

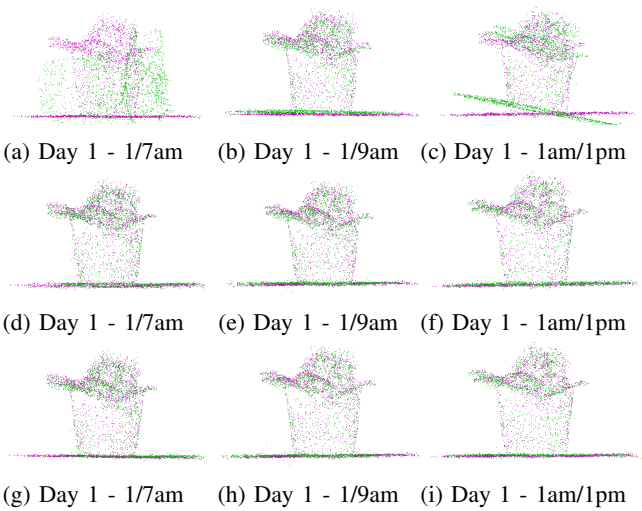

(a) Day 1 - 1/7am (b) Day 1 - 1/9am (c) Day 1 - 1am/1pm

(d) Day 1 - 1/7am (e) Day 1 - 1/9am (f) Day 1 - 1am/1pm

(g) Day 1 - 1/7am (h) Day 1 - 1/9am (i) Day 1 - 1am/1pm

Fig. 6: An example of the spatio-temporal registration of the point clouds from the violet dataset using the pairwise registration. Top row: *(a)*, *(b)* and *(c)* show the results for three example pairs under the 6 DoF transformation. Middle row: *(d)*, *(e)* and *(f)* show the results for three example pairs under the 7 DoF transformation. Bottom row: *(g)*, *(h)* and *(i)* show the results for three example pairs under the 9 DoF transformation. The source and target point clouds are respectively differentiated in violet and green color.

optimization stage, we bundle temporal point clouds of a sliding window size, fix the coordinate of the first point cloud, and estimate the transformations that best register the remaining clouds in the bundle. We then move to the next optimization bundle by a gap size. Bigger sliding window and smaller gap size is the optimal choice, but it comes with computation burdens. We empirically retained a window size of 10 (models) and a gap of 5 (models) for the results presented in this paper. The optimization phase uses the point correspondences between models within the sliding window and minimizes the following objective function:

$$J = \min_{r,t,s} \sum_{(i,j)\in\mathcal{P}} \rho(P_j - {}^{w}H_j^{-1} \times {}^{w}H_i \times P_i) \quad (5)$$

where P_i and P_j are the corresponding 3D points in the source and target point clouds within the bundle. The indices i, and j belong to all possible pairs $\mathcal{P}$ within the bundle. The parameters of the optimization: r, t, s, are the rotation, translation, and scale of each model with respect to a global coordinate frame. At each optimization phase (Eq. 5) the first model parameters are excluded from the optimization leaving $(SW-1)\times DoF$ parameters for the optimization. The $\rho(.)$ is a robust penalty function to reject outliers. The Graduated Non-Convexity (GNC) approach [43] is used to solve the non-convex optimization problem.

V. Experimental Evaluation

The evaluation of non-rigid registration methods is not straight-forward and visual assessments have been used over the years [9]. In this paper, the experiments were designed to qualitatively and quantitatively evaluate the proposed spatio-temporal registration pipeline on the African violet dataset. For qualitative evaluation, we conduct a visual assessment of the registration results and also visualize the time-series models using VisND [15]. For quantitative evaluation, we used the registration error between the source P_s and target P_t point clouds as defined in the following equation:

$$E = \frac{1}{K}\sum_{k=1}^{K} \|p_1^i - p_2^j\| \quad (6)$$

where: E is the registration error, K is the number of vertices in P_s, p_2^j is the vertex in P_t that is the closest to the vertex p_1^i in P_s.

In order to show the performance of the proposed approach, the experiments were based on three approaches: pairwise, incremental and bundle registrations. For each approach, three types of transformations were evaluated under 6 (3 translations and 3 rotations), 7 (3 translations, 3 rotations and 1 scale) and 9 DoF (3 translations, 3 rotations and 3 scales) to appreciate the effectiveness of the proposed approach in the presence of scale during the registration of time lapsed 3D point clouds.

A. Pairwise registration

We applied a pairwise registration to align all the temporal 3D models with respect to the first 3D Model generated in day 1 taken as the global coordinate frame. Figure 6 illustrates the results of the pairwise registration for three example pairs of point clouds under 6, 7 and 9 DoF transformations.

B. Incremental registration

We applied an incremental registration to the point clouds. In this approach, consecutive pairs of point clouds were registered at a time. By incrementally registering the models, we propagating the transformations from the initial to the final models. The downside of this method is that the error also propagated throughout the temporal registration when more models were added. Figure 7 illustrates the results of the incremental registration for three example pairs of point clouds under 6, 7 and 9 DoF transformations.

C. Bundle registration

We applied the bundle registration of the point clouds as explained in the proposed methodology in section IV. We empirically retained a window size of 10 and a gap size of 5 for the results presented here. We show that the bundle registration is able to handle the presence of noise, outliers and different level of overlaps in the 3D point clouds. Figure 8 illustrates the results of the bundle registration for three example pairs of point clouds under 6, 7 and 9 DoF transformations.

In Table I, we report the average registration errors for all three approaches based on the different transformations over the entire African violet dataset.We obtained an average

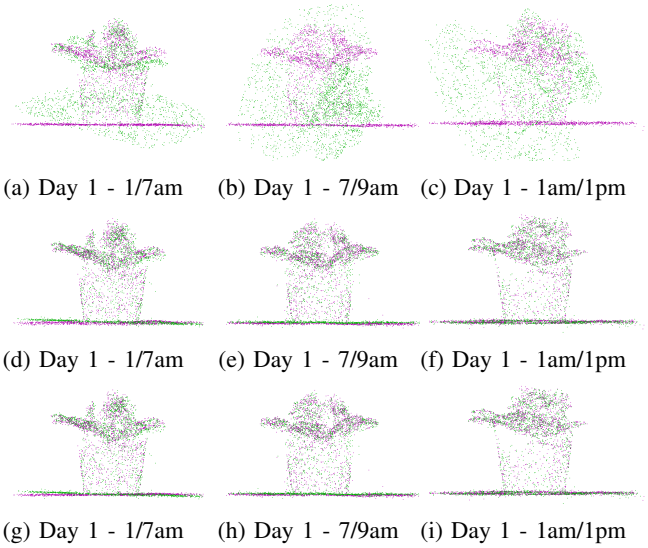

(a) Day 1 - 1/7am (b) Day 1 - 7/9am (c) Day 1 - 1am/1pm

(d) Day 1 - 1/7am (e) Day 1 - 7/9am (f) Day 1 - 1am/1pm

(g) Day 1 - 1/7am (h) Day 1 - 7/9am (i) Day 1 - 1am/1pm

Fig. 7: An example of the spatio-temporal registration of the point clouds from the violet dataset using the incremental registration. Top row: *(a)*, *(b)* and *(c)* show the results three example pairs under the 6 DoF transformation. Middle row: *(d)*, *(e)* and *(f)* show the results for three example pairs under the 7 DoF transformation. Bottom row: *(g)*, *(h)* and *(i)* show the results for three example pairs under the 9 DoF transformation. The source and target point clouds are respectively differentiated in violet and green color.

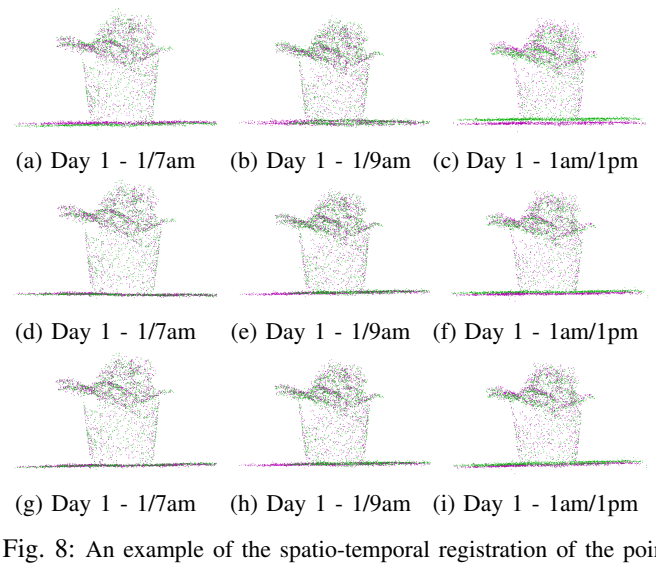

(a) Day 1 - 1/7am (b) Day 1 - 1/9am (c) Day 1 - 1am/1pm

(d) Day 1 - 1/7am (e) Day 1 - 1/9am (f) Day 1 - 1am/1pm

(g) Day 1 - 1/7am (h) Day 1 - 1/9am (i) Day 1 - 1am/1pm

Fig. 8: An example of the spatio-temporal registration of the point clouds from the violet dataset using the bundle registration. Top row: *(a)*, *(b)* and *(c)* show the results for three example pairs under the 6 DoF transformation. Middle row: *(d)*, *(e)* and *(f)* show the results for three example pairs under the 7 DoF transformation. Bottom row: *(g)*, *(h)* and *(i)* show the results for three example pairs under the 9 DoF transformation. The source and target point clouds are respectively differentiated in violet and green color.

error of less than $2mm$ with all the transformations using the proposed bundle registration approach, which indicates the effectiveness of the method. Although, the registration errors for the pairwise and bundle approaches are close for the proposed dataset, the pairwise approach will fail if the amount of change is high between frames (e.g. for growth plants observed during longer period of time). In Figure 9, we compare the average daily registration errors over ten days under 6, 7 and 9DoF transformations.

D. VisND

We used VisND [15], a multidimensional visualization tool for plant phenotyping, to visualize the aligned spatio-temporal 3D models. The tool allowed us to effectively visualize the temporal changes occurring during the plant development over time by playing sequences of aligned time-series point clouds as a video. Figure 10 presents four VisND snapshots of the visualization of spatio-temporal 3D models of the African violet plant. In addition, with VisND, the point cloud can be manipulated to inspect and get additional information about the plant at each specific time frame. It is a tool that can be used to visualize, extract, analyze, monitor and track over time multidimensional datasets in various fields.

VI. Conclusion

This paper introduced a new multi-view stereo dataset made of temporal stereo raw images and processed spatio-temporal 3D models of an African violet. The plant was observed over ten days of the blooming of its flowers. Furthermore, we

TABLE I: Average errors for each time-series registration approach with the African violet dataset under 6, 7 and 9 DoF transformations. The values in the table are expressed in millimeter (mm).

Approach	6DoF	7DoF	9DoF
Pairwise	10.7459	1.5951	1.5878
Incremental	36.7156	3.7012	3.7856
Bundle	**1.7364**	**1.5778**	**1.5862**

presented a bundle registration algorithm for spatio-temporal 3D point clouds. For the experimental evaluations, we applied three different spatio-temporal registration approaches on the proposed dataset: pairwise, incremental and bundle registrations under 6 (3 rotations and 3 translations), 7 (3 rotations, 3 translations and 1 scale) and 9 (3 rotations, 3 translations and 3 scales) DoF transformations. We showed that the proposed bundle registration algorithm performs better than the pairwise and incremental approaches, and can handle the changes in rotation, translation and scale due to the anisotropic growth of the plant. The registered spatio-temporal 3D point clouds were evaluated quantitatively by computing the registration error, and qualitatively using VisND, which is an N-dimensional open-source visualization tool for temporal datasets. Future directions for this paper include addressing the drawbacks of the SOTA descriptors investigated in the 3D registration step (e.g., PFH, FPFH, and PFHRGB). In particular, we believe that including Local-to-Global Signature (LGS) [44] 3D descriptor in the current pipeline, could provide even lower registration errors.

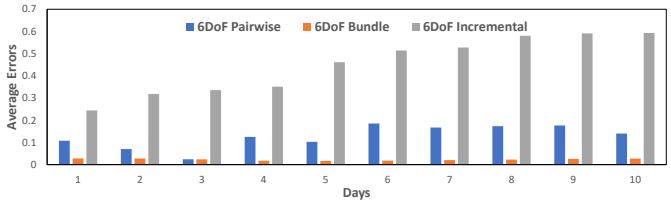

(a) Average error for 6DoF transformation

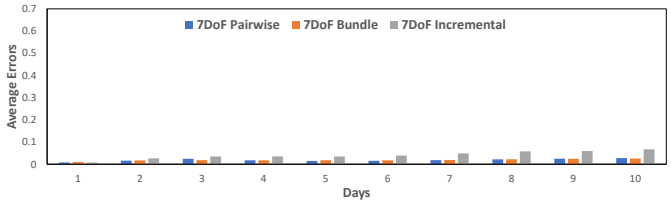

(b) Average error for 7DoF transformation

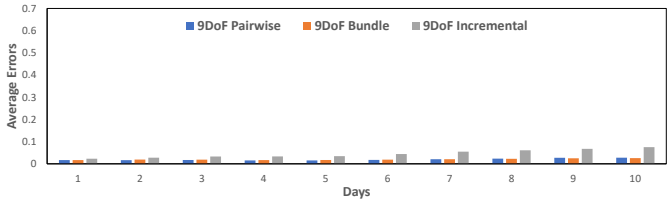

(c) Average error for 9DoF transformation

Fig. 9: A comparison of average daily registration errors between all the registration methods over 10 days for *(a)* 6, *(b)* 7 and *(c)* 9DoF transformations.

REFERENCES

[1] R. Pieruschka, U. Schurr *et al.*, "Plant phenotyping: past, present, and future," *Plant Phenomics*, vol. 2019, p. 7507131, 2019.

[2] A. Walter, F. Liebisch, and A. Hund, "Plant phenotyping: from bean weighing to image analysis," *Plant methods*, vol. 11, no. 1, p. 14, 2015.

[3] H. Scharr, H. Dee, A. P. French, and S. A. Tsaftaris, "Special issue on computer vision and image analysis in plant phenotyping," 2016.

[4] M. Minervini, H. Scharr, and S. A. Tsaftaris, "Image analysis: the new bottleneck in plant phenotyping [applications corner]," *IEEE signal processing magazine*, vol. 32, no. 4, pp. 126–131, 2015.

[5] A. Shafiekhani, S. Kadam, F. B. Fritschi, and G. N. DeSouza, "Vinobot and vinoculer: two robotic platforms for high-throughput field phenotyping," *Sensors*, vol. 17, no. 1, p. 214, 2017.

[6] F. Golbach, G. Kootstra, S. Damjanovic, G. Otten, and R. van de Zedde, "Validation of plant part measurements using a 3d reconstruction method suitable for high-throughput seedling phenotyping," *Machine Vision and Applications*, vol. 27, no. 5, pp. 663–680, 2016.

[7] T. T. Santos and G. C. Rodrigues, "Flexible three-dimensional modeling of plants using low-resolution cameras and visual odometry," *Machine Vision and Applications*, vol. 27, no. 5, pp. 695–707, 2016.

[8] M. P. Pound, A. P. French, J. A. Fozard, E. H. Murchie, and T. P. Pridmore, "A patch-based approach to 3d plant shoot phenotyping," *Machine Vision and Applications*, vol. 27, no. 5, pp. 767–779, 2016.

[9] G. K. Tam, Z.-Q. Cheng, Y.-K. Lai, F. C. Langbein, Y. Liu, D. Marshall, R. R. Martin, X.-F. Sun, and P. L. Rosin, "Registration of 3d point clouds and meshes: A survey from rigid to nonrigid," *IEEE transactions on visualization and computer graphics*, vol. 19, no. 7, pp. 1199–1217, 2012.

[10] A. Shafiekhani, F. B. Fritschi, and G. N. DeSouza, "A new 4d-rgb mapping technique for field-based high-throughput phenotyping." in *BMVC*, 2018, p. 322.

[11] A. Shafiekhani, "Spatio-temporal acquisition, reconstruction, and visualization of dynamic scenes for plant phenotyping," Ph.D. dissertation, University of Missouri-Columbia, 2020.

[12] N. Chebrolu, T. Läbe, and C. Stachniss, "Spatio-temporal non-rigid registration of 3d point clouds of plants," in *2020 IEEE International Conference on Robotics and Automation (ICRA)*. IEEE, 2020, pp. 3112–3118.

[13] N. Chebrolu, F. Magistri, T. Läbe, and C. Stachniss, "Registration of spatio-temporal point clouds of plants for phenotyping," *PloS one*, vol. 16, no. 2, p. e0247243, 2021.

[14] J. Dong, J. G. Burnham, B. Boots, G. Rains, and F. Dellaert, "4d crop monitoring: Spatio-temporal reconstruction for agriculture," in *2017 IEEE International Conference on Robotics and Automation (ICRA)*. IEEE, 2017, pp. 3878–3885.

[15] A. Shafiekhani, F. B. Fritschi, and G. N. DeSouza, "Visnd: A visualization tool for multidimensional model of canopy," in *Proceedings of the IEEE/CVF Conference on Computer Vision and Pattern Recognition Workshops*, 2019.

[16] B. Bellekens, V. Spruyt, R. Berkvens, and M. Weyn, "A survey of rigid 3d pointcloud registration algorithms," in *AMBIENT 2014: the Fourth International Conference on Ambient Computing, Applications, Services and Technologies, August 24-28, 2014, Rome, Italy*, 2014, pp. 8–13.

[17] H. Laga, "A survey on nonrigid 3d shape analysis," in *Academic Press Library in Signal Processing, Volume 6*. Elsevier, 2018, pp. 261–304.

[18] M. A. Audette, F. P. Ferrie, and T. M. Peters, "An algorithmic overview of surface registration techniques for medical imaging," *Medical image analysis*, vol. 4, no. 3, pp. 201–217, 2000.

[19] O. Van Kaick, H. Zhang, G. Hamarneh, and D. Cohen-Or, "A survey on shape correspondence," in *Computer Graphics Forum*, vol. 30, no. 6. Wiley Online Library, 2011, pp. 1681–1707.

[20] S. Marden and J. Guivant, "Improving the performance of icp for real-time applications using an approximate nearest neighbour search," in *Proceedings of Australasian Conference on Robotics and Automation*, 2012, pp. 3–5.

[21] W. S. Yambor, B. A. Draper, and J. R. Beveridge, "Analyzing pca-based face recognition algorithms: Eigenvector selection and distance measures," in *Empirical evaluation methods in computer vision*. World Scientific, 2002, pp. 39–60.

[22] P. J. Besl and N. D. McKay, "Method for registration of 3-d shapes," in *Sensor fusion IV: control paradigms and data structures*, vol. 1611. International Society for Optics and Photonics, 1992, pp. 586–606.

[23] S. Fantoni, U. Castellani, and A. Fusiello, "Accurate and automatic alignment of range surfaces," in *2012 Second International Conference on 3D Imaging, Modeling, Processing, Visualization & Transmission*. IEEE, 2012, pp. 73–80.

[24] A. Segal, D. Haehnel, and S. Thrun, "Generalized-icp." in *Robotics: science and systems*, vol. 2, no. 4. Seattle, WA, 2009, p. 435.

[25] D. Haehnel, S. Thrun, and W. Burgard, "An extension of the icp algorithm for modeling nonrigid objects with mobile robots," in *IJCAI*, vol. 3, 2003, pp. 915–920.

[26] D. Rueckert, L. I. Sonoda, C. Hayes, D. L. Hill, M. O. Leach, and D. J. Hawkes, "Nonrigid registration using free-form deformations: application to breast mr images," *IEEE transactions on medical imaging*, vol. 18, no. 8, pp. 712–721, 1999.

[27] P. Safayenikoo, A. Asad, M. Fathy, and F. Mohammadi, "An energy efficient non-uniform last level cache architecture in 3d chip-multiprocessors," in *2017 18th International Symposium on Quality Electronic Design (ISQED)*. IEEE, 2017, pp. 373–378.

[28] B. Amberg, S. Romdhani, and T. Vetter, "Optimal step nonrigid icp algorithms for surface registration," in *2007 IEEE Conference on Computer Vision and Pattern Recognition*. IEEE, 2007, pp. 1–8.

[29] F. Endres, J. Hess, N. Engelhard, J. Sturm, D. Cremers, and W. Burgard, "An evaluation of the rgb-d slam system," in *2012 IEEE International Conference on Robotics and Automation*. IEEE, 2012, pp. 1691–1696.

[30] S. Das Choudhury, S. Goswami, S. Bashyam, A. Samal, and T. Awada, "Automated stem angle determination for temporal plant phenotyping analysis," in *Proceedings of the IEEE International Conference on Computer Vision Workshops*, 2017, pp. 2022–2029.

[31] Y. Li, X. Fan, N. J. Mitra, D. Chamovitz, D. Cohen-Or, and B. Chen, "Analyzing growing plants from 4d point cloud data," *ACM Transactions on Graphics (TOG)*, vol. 32, no. 6, pp. 1–10, 2013.

[32] A. Paproki, X. Sirault, S. Berry, R. Furbank, and J. Fripp, "A novel mesh processing based technique for 3d plant analysis," *BMC plant biology*, vol. 12, no. 1, p. 63, 2012.

[33] J. L. Schönberger, E. Zheng, M. Pollefeys, and J.-M. Frahm, "Pixelwise view selection for unstructured multi-view stereo," in *European Conference on Computer Vision (ECCV)*, 2016.

[34] J. L. Schönberger and J.-M. Frahm, "Structure-from-motion revisited," in *Conference on Computer Vision and Pattern Recognition (CVPR)*, 2016.

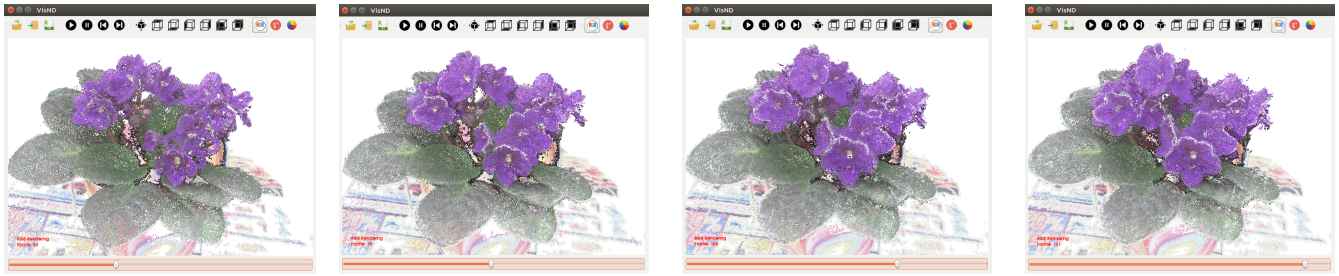

(a) Frame 50 (b) Frame 70 (c) Frame 100 (d) Frame 130

Fig. 10: Snapshots of VisND with Spatio-temporal 3D models of the African violet.

[35] H. Huang, S. Wu, D. Cohen-Or, M. Gong, H. Zhang, G. Li, and B. Chen, "L1-medial skeleton of point cloud." *ACM Trans. Graph.*, vol. 32, no. 4, pp. 65–1, 2013.

[36] I. Sipiran and B. Bustos, "Harris 3d: a robust extension of the harris operator for interest point detection on 3d meshes," *The Visual Computer*, vol. 27, no. 11, p. 963, 2011.

[37] L. A. Alexandre, "3d descriptors for object and category recognition: a comparative evaluation," in *Workshop on Color-Depth Camera Fusion in Robotics at the IEEE/RSJ International Conference on Intelligent Robots and Systems (IROS), Vilamoura, Portugal*, vol. 1, no. 3, 2012, p. 7.

[38] X.-F. Hana, J. S. Jin, J. Xie, M.-J. Wang, and W. Jiang, "A comprehensive review of 3d point cloud descriptors," *arXiv preprint arXiv:1802.02297*, 2018.

[39] R. Hänsch, T. Weber, and O. Hellwich, "Comparison of 3d interest point detectors and descriptors for point cloud fusion," *ISPRS Annals of the Photogrammetry, Remote Sensing and Spatial Information Sciences*, vol. 2, no. 3, p. 57, 2014.

[40] R. B. Rusu, N. Blodow, Z. C. Marton, and M. Beetz, "Aligning point cloud views using persistent feature histograms," in *2008 IEEE/RSJ International Conference on Intelligent Robots and Systems*. IEEE, 2008, pp. 3384–3391.

[41] R. B. Rusu, N. Blodow, and M. Beetz, "Fast point feature histograms (fpfh) for 3d registration," in *2009 IEEE international conference on robotics and automation*. IEEE, 2009, pp. 3212–3217.

[42] R. B. Rusu and S. Cousins, "3d is here: Point cloud library (pcl)," in *2011 IEEE international conference on robotics and automation*. IEEE, 2011, pp. 1–4.

[43] A. Blake and A. Zisserman, *The Graduated Non-Convexity Algorithm*. MIT Press, 2003, pp. 131–166.

[44] I. Hadji and G. N. DeSouza, "Local-to-global signature descriptor for 3d object recognition," in *Asian conference on computer vision*. Springer, 2014, pp. 570–584.